

# Exploring the Magnus expansion and the in-medium similarity renormalization group

A. J. Tropiano<sup>1</sup>, S. K. Bogner<sup>2</sup>, R. J. Furnstahl<sup>1</sup>

<sup>1</sup>*Department of Physics, The Ohio State University, Columbus, OH 43210, USA*

<sup>2</sup>*National Superconducting Cyclotron Laboratory and Department of Physics and Astronomy,  
Michigan State University, East Lansing, MI 48824, USA*

(Dated: April 10, 2019)

## Abstract

- Test Magnus expansion SRG implementation on LO NN potential at high  $\Lambda$ . (Define SRG or IMSRG acronym in abstract.)
- High  $\Lambda$  leads to spurious bound states in spin triplet channels.
- Decouple spurious bound state(s) by using two approaches within the Magnus implementation to drive the Hamiltonian to band-diagonal, unitarily equivalent form.
- One choice of generator where the deep bound state is decoupled outside low-momentum and another where it is shifted to low-momentum.
- Deep bound state corrupts low-momentum physics.
- Connection to IMSRG intruder state problem.
- Confirm unitarity of Hamiltonian by evaluation of deuteron observables.
- Lastly, study operator evolution.

## I. INTRODUCTION

- In recent years *ab initio* methods have made strides in nuclear structure and reactions.
- Realistic binding energies starting from NN and 3N forces have been calculated for many medium mass nuclei using different many-body methods.
- The in-medium similarity renormalization group (IMSRG) is one such method [1, 2].
- The IMSRG separates energy scales in the nuclear Hamiltonian by decoupling the reference state from excited states to band- or block-diagonal form.
- One can use the decoupled Hamiltonian to solve the many-body Schrödinger equation extracting specific eigenvalues and eigenstates which qualifies the IMSRG as an *ab initio* method.
- The IMSRG procedure requires solving a system of nonlinear, coupled differential equations which can often be stiff necessitating a high-order ODE solver.
- In principle, the decoupled Hamiltonian (or any operator) is unitarily equivalent but the numerical error of solving the ODE can lead to error on observable quantities.
- Furthermore, the model spaces for IMSRG calculations can be extremely large.
- Evolving several operators is often impossible due to memory restrictions in storing several operators.
- A variant of the IMSRG that utilizes the Magnus expansion can overcome these limitations.
- We will refer to this as the Magnus implementation or simply Magnus.
- The Magnus solves for the unitary transformation directly whereas the IMSRG applies the transformation indirectly in steps of the differential flow equation.
- From the form of the transformation, the numerical error leaves the unitarity of the evolved Hamiltonian un-affected.
- By explicitly solving for the transformation, one can evolve several operators.
- The Magnus implementation has become a standard technique in IMSRG calculations as studies have targeted observables such as radii, electromagnetic moments and transitions, etc., requiring consistently evolved operators.

- We test the Magnus implementation on chiral non-local NN potentials in free-space for several EFT cutoffs.
  - At high cutoffs, spin triplet channels feature spurious, deeply bound states from the strong, repulsive tensor force [5].
  - These bound states are features of high-momentum physics and lie outside the range of the EFT.
  - However, potentials with deeply bound states have shown sensitivity to SRG transformations [6, 7].
  - Details of the SRG transformation can cause the spurious bound state(s) to corrupt the low-momentum physics.
  - An analogous problem occurs in IMSRG calculations for systems with intruder states where the intruder state can shift to the energy scale of the reference state in valence space.
  - This severely distorts low-energy properties such as the ground state wave function.
  - It is not understood how the IMSRG procedure evolves intruder state systems.
  - Due to the prominence of the Magnus in IMSRG, one must first understand if the Magnus approach matches the typical approach for difficult systems before investigating the intruder state problem.
  - NN potentials with spurious bound states offer a good test laboratory for the Magnus implementation to better understand if the Magnus is equivalent to the SRG approach.
- 
- The past decade has seen a tremendous increase in the number of chiral NN potentials.
  - Interactions can now be built up to N5LO and feature several different regularization schemes.
  - A natural question is to ask whether the SRG decouples these potentials in the same way.
  - There is evidence of universal, low-momentum matrix elements as seen from evolving different potentials with SRG transformations or  $V_{low\ k}$  [4].
  - There has also been renewed interest in chiral potentials at high-cutoffs but for a locally regulated potential [8].
  - Given the growing number of chiral interactions, it would be interesting to re-examine these areas from an SRG standpoint.
  - However, we would like to focus on a fixed comparison of the SRG and the Magnus approach as a first test, and therefore only consider evolving non-local LO NN potentials at

various cutoffs.

- We leave the other areas as topics for future studies.
- The rest of the paper is organized as follows:
- In Sec. II we review the formalism of the SRG and the Magnus implementation emphasizing the major advantages of the Magnus.
- In Sec. III we test the Magnus implementation on high-cutoff NN potentials.
- We briefly review the SRG results for the same set of bare interactions and compare Magnus to SRG results.
- With the Magnus evolved operators, we calculate several observables and explore operator evolution.
- Lastly, we summarize our results in Sec. IV.
- We discuss the implications for the Magnus expansion within the IMSRG.

## II. FORMALISM

### SRG formalism

- In this section we describe the SRG in the context of decoupling any operator.
- The SRG decouples low- and high-momentum scales by applying a continuous unitary transformation  $U(s)$  where  $s = 0 \rightarrow \infty$  is the flow parameter.
- The ‘dressed’ or evolved operator is given by

$$O(s) = U(s)O(0)U^\dagger(s), \quad (1)$$

where  $O(0)$  corresponds to the ‘bare’ operator.

- Because  $U(s)$  is unitary, the observables of the operator are preserved.
- In practice, the unitary transformation  $U(s)$  is not explicitly solved for; the evolved operator is given by a differential flow equation which is obtained by taking the derivative of Eqn. (1),

$$\frac{dO(s)}{ds} = [\eta(s), O(s)], \quad (2)$$

where  $\eta(s) = \frac{dU(s)}{ds}U^\dagger(s) = -\eta^\dagger(s)$  is the anti-hermitian SRG generator.

- The generator is defined as a commutator,

$$\eta(s) = [G, H(s)], \quad (3)$$

where  $G$  specifies the type of flow or form of the decoupled operator.

- To drive the operator to band-diagonal form, set  $G = H_D(s)$ , the diagonal of the Hamiltonian.
- This choice was implemented by Wegner in condensed matter physics [9].
- For notational convenience, we write the Wegner choice without the  $s$  dependence in the rest of the paper.
- In a similar option used in nuclear physics,  $G$  is set to the relative kinetic energy,  $T_{rel}$ , which also drives to band-diagonal form.
- In this paper, we consider both choices.
- Generally the flow equation (2) is solved up to some finite value of  $s$  with a high-order ODE solver.
- It is convenient to define  $\lambda \equiv s^{-1/4}$  which roughly measures the width of the diagonal in the decoupled operator.

### Magnus expansion formalism

- We now consider the Magnus implementation.
- Mathematically speaking, the Magnus expansion is a method for solving an initial value problem associated with a linear ordinary differential equation (ODE).
- Formal details of the Magnus expansion are discussed in [10].
- We will introduce the Magnus expansion in the context of SRG evolving any operator.
- In an intermediate step in deriving Eqn. (2), we have a linear ODE for  $U(s)$ ,

$$\frac{dU(s)}{ds} = \eta(s)U(s). \quad (4)$$

- Magnus showed that one can solve the following equation with a solution  $U(s) = e^{\Omega(s)}$  where  $\Omega(s)$  is expanded as a power series,  $\sum_n \Omega_n$  (referred to as the Magnus expansion or Magnus series).
- The terms of the series are given by integral expressions involving  $\eta(s)$  (again, see [10, 11] for details).
- For our case, we focus on the formally exact derivative of  $\Omega(s)$ ,

$$\frac{d\Omega(s)}{ds} = \sum_{k=0}^{\infty} \frac{B_k}{k!} ad_{\Omega}^k(\eta), \quad (5)$$

where  $B_k$  are the Bernoulli numbers,  $ad_{\Omega}^0(\eta) = \eta(s)$ , and  $ad_{\Omega}^k(\eta) = [\Omega(s), ad_{\Omega}^{k-1}(\eta)]$ .

- We integrate this differential equation to find  $\Omega(s)$  and evaluate the unitary transformation

directly.

- Then the evolved operator can be evaluated with the BCH formula:

$$O(s) = e^{\Omega(s)} O e^{-\Omega(s)} = \sum_{k=0}^{\infty} \frac{1}{k!} \text{ad}_{\Omega}^k(O). \quad (6)$$

- As  $k \rightarrow \infty$  in both sums in Eqns. (5) and (6) the Magnus transformation matches the SRG transformation.

- We investigate several truncations  $k_{max}$  in Eqn. (5) and take many terms,  $k_{max} \sim 25$ , in Eqn. (6).

– Here or earlier (for the following bullets)? Better to motivate the Magnus in the introduction or easier to explain given mathematical detail?

- There are significant advantages in the Magnus implementation.
- In the typical approach, the numerical error associated with solving the flow equation affects the accuracy of the observables for the evolved operator.
- Therefore, one must use a high-order ODE solver in integrating the flow equation (2).
- In the Magnus implementation, unitarity is guaranteed by the form of  $U(s)$ ; in fact, one could solve Eqn. (5) with a simple first-order Euler step-method keeping the same observables while decoupling the operator as desired.
- This offers a decent computational speed-up by avoiding a high-order solver.
- In this paper, we demonstrate this advantage by applying the Magnus implementation using the first-order Euler step-method.
- The second major advantage involves the evolution of multiple operators.
- In many other situations, one may be interested in evolving several operators at a time.
- In the SRG procedure, we would have another set of coupled equations in Eqn. (2), drastically increasing memory usage.
- Each additional operator increases the set of equations - say  $N$  equations - by another factor of  $N$ .
- In the Magnus, one only needs  $\Omega(s)$  to consistently evolve several operators.
- We avoid the cost in memory by directly constructing  $U(s) = e^{\Omega(s)}$ .
- This is especially useful in IMSRG calculations where the model space can be very large.
- In the next section, we discuss results from Magnus evolved large-cutoff potentials focusing on the flow of the potential, observables, and operator evolution.

### III. RESULTS

#### Evolution of potentials

- In this section, we Magnus evolve LO non-local potentials in the  ${}^3S_1 - {}^3D_1$  channel at cutoffs of  $\Lambda = 4, 9$ , and  $20 \text{ fm}^{-1}$ .
- **Option: add new regularization schemes?**
- For the higher two cutoffs, the potentials have one and two spurious, deeply bound states, respectively.
- In [7], potentials at large-cutoffs were SRG evolved with  $G = H_D$  and  $G = T_{rel}$ .
- At lower cutoffs ( $\Lambda \lesssim 4 \text{ fm}^{-1}$ ), potential matrix elements flowed toward a decoupled, universal form independent of  $G$ , that is the low-momentum matrix elements approached the same values as  $\lambda \rightarrow 0$ .
- However, SRG evolution differed for potentials featuring one or more spurious bound states.
- With one or more spurious bound states and  $G = T_{rel}$ , the SRG transformation shifted a spurious bound state toward the low-momentum block corrupting the low-energy physics (e.g., the deuteron wave function, phase shifts, etc.).
- For  $G = H_D$ , the SRG decoupled the spurious bound state outside the low-momentum block matching the flow to universal low-momentum form independent of the cutoff  $\Lambda$ .
- Similar behavior could be prevalent in IMSRG calculations where the choice in generator affects evolution of many-body Hamiltonians with intruder states as it does for these NN potentials in free-space SRG.
  
- First, we compare Magnus to SRG evolution for large cutoff potentials with  $G = H_D$  and  $G = T_{rel}$ .
- Figures 1 and 2 show potential matrix element evolution for three truncations in the sum of Eqn. 5 up to three values of  $\lambda$  with  $\Lambda = 9 \text{ fm}^{-1}$ .
- At this cutoff, the potential has one spurious bound state at about  $-2000 \text{ MeV}$ .
  - We see the same behavior with the Magnus in comparison to the SRG in [7] for both generators.
- For  $G = H_D$ , there is a deep, blue dot in the middle of the contours at  $k \approx 1.75 \text{ fm}^{-1}$  which corresponds to the decoupled spurious bound state.

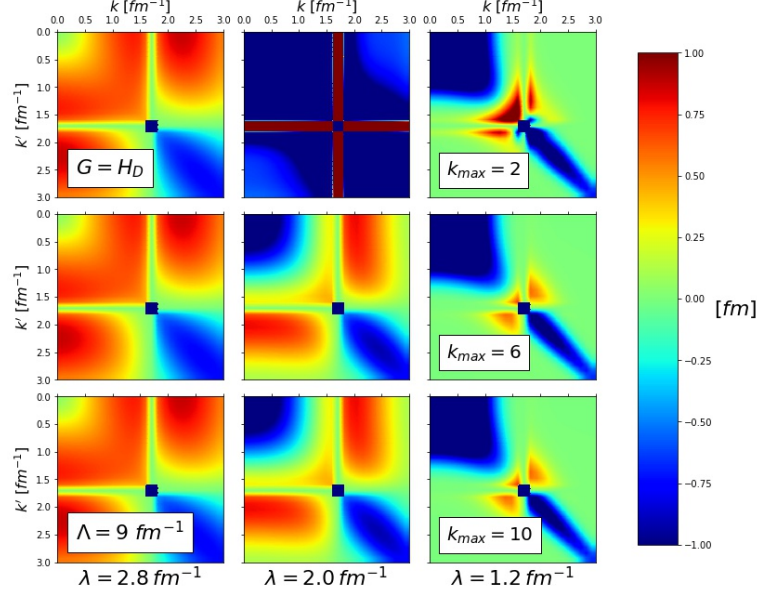


FIG. 1: Contours of Magnus evolved  $V_\lambda(k, k')$  with  $\Lambda = 9 \text{ fm}^{-1}$  and  $G = H_D$  for  $\lambda = 2.8$  (left),  $2.0$  (middle), and  $1.2$  (right)  $\text{fm}^{-1}$  and truncations in the Magnus  $k_{max} = 2$  (top),  $6$  (middle), and  $10$  (bottom).

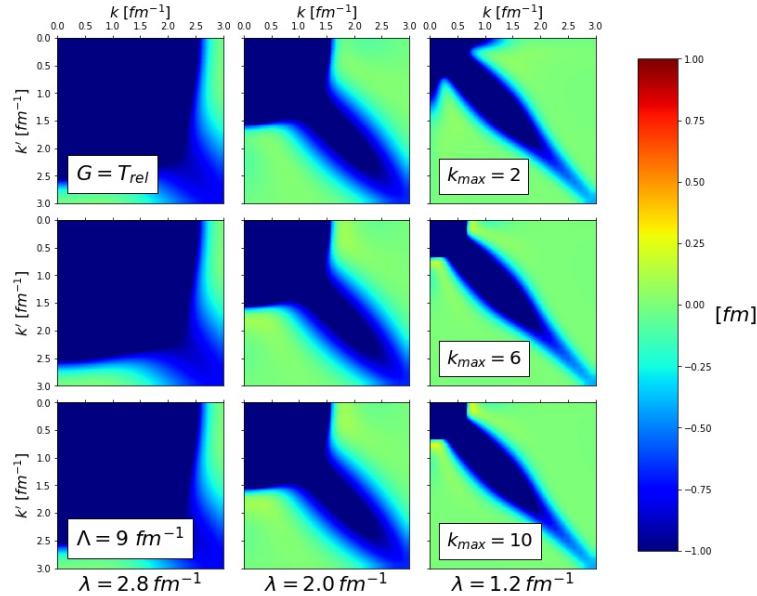


FIG. 2: Contours of Magnus evolved  $V_\lambda(k, k')$  with  $\Lambda = 9 \text{ fm}^{-1}$  and  $G = T_{rel}$  for  $\lambda = 2.8$  (left),  $2.0$  (middle), and  $1.2$  (right)  $\text{fm}^{-1}$  and truncations in the Magnus  $k_{max} = 2$  (top),  $6$  (middle), and  $10$  (bottom).



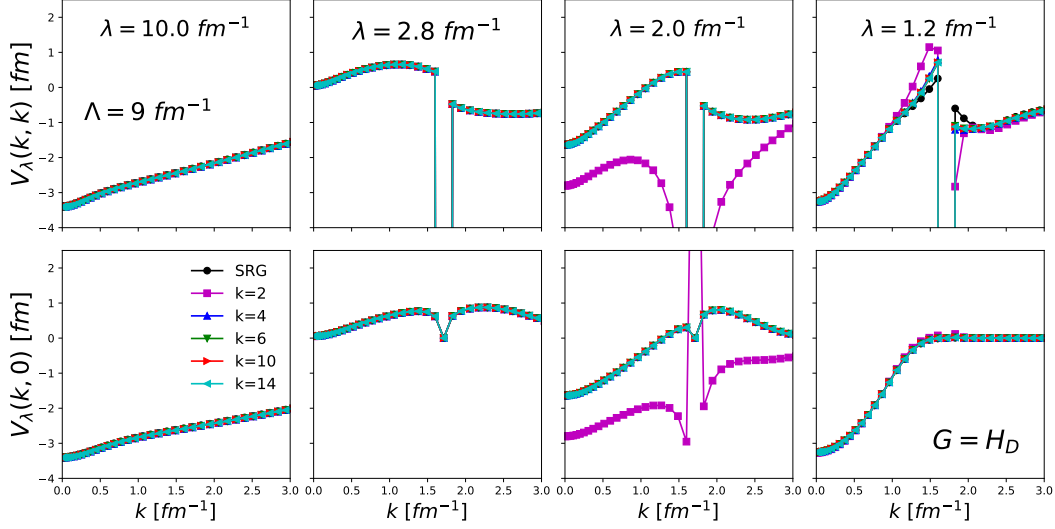


FIG. 3: Diagonal (top row) and far off-diagonal (bottom row) matrix elements of evolved  $V_\lambda(k, k')$  with  $\Lambda = 9 \text{ fm}^{-1}$  and  $G = H_D$  for several values of  $\lambda$  and truncations in the Magnus series  $k_{max}$ .

- We have checked other cutoffs and found that the evolved low-momentum matrix elements are independent of the cutoff  $\Lambda$  implying a low-momentum, universal form.
- The only major difference in Magnus or SRG evolution for various cutoffs is where spurious bound state(s) are decoupled.
- This decoupling feature depends on the details of the starting interaction (i.e., the value of the bound state).
  - Furthermore, it is dependent on the momentum mesh on which the potential is generated.
- At  $k_{max} = 2$  and  $\lambda = 2.0 \text{ fm}^{-1}$ , we see large, positive off-diagonal values along the momentum axes where the deep bound state is decoupled.
- Solving for  $\Omega(s)$  at a low truncation leads to less desirable flow, that is, the transformation  $U(s)$  is not quite the same transformation as the SRG  $U(s)$ .
- However, the Magnus still guarantees the unitarity of  $U(s)$ , and we see a consistent decoupling of the spurious bound state in each row independent of  $k_{max}$ .
- For  $G = T_{rel}$ , the spurious bound state is shifted up along the diagonal, and the low-momentum block drops to extremely negative values.
- Here, the spurious bound state corrupts the low-momentum block matching the SRG evolution of different cutoffs, thus breaking universality.
  - Figures 3 and 4 show a more quantitative depiction of the evolved potentials.
  - The black dotted line corresponds to the SRG evolved potential whereas the other lines

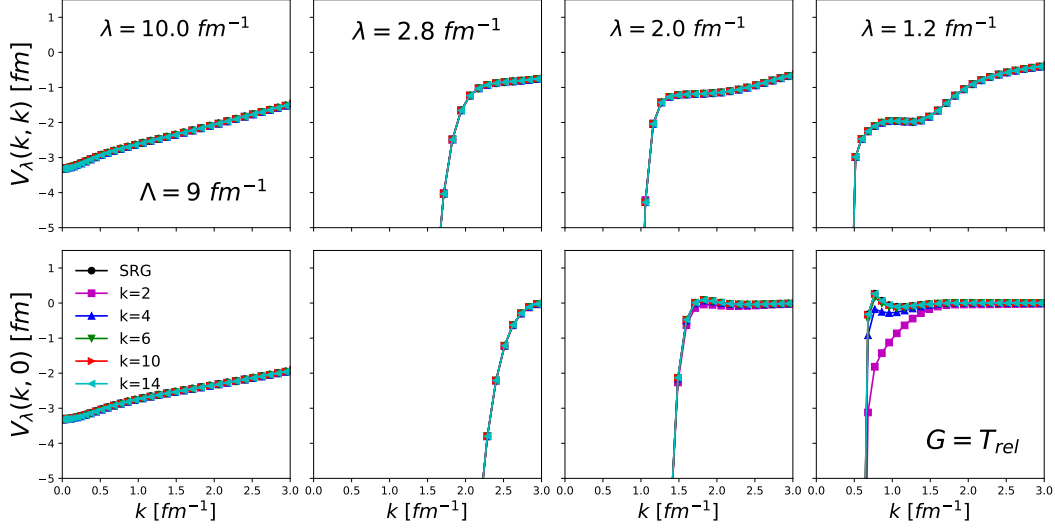


FIG. 4: Diagonal (top row) and far off-diagonal (bottom row) matrix elements of evolved  $V_\lambda(k, k')$  with  $\Lambda = 9 \text{ fm}^{-1}$  and  $G = T_{rel}$  for several values of  $\lambda$  and truncations in the Magnus series  $k_{max}$ .

are Magnus evolved potentials for different  $k_{max}$  for diagonal and far-off diagonal matrix elements of  $V_\lambda(k, k')$ .

- It is clear in these figures that the Magnus matches the SRG at  $k_{max} \gtrsim 6$ .
- In Figure 3 the decoupled spurious bound state is seen as the large negative drop in the curves at  $k \approx 1.75 \text{ fm}^{-1}$ .
- Unnecessary?
- From applying the Magnus in several other cases, we have seen that harder potentials cause convergence issues in the Magnus expansion due to the relative size of the SRG generator  $\eta(s)$ .
- To avoid convergence issues we can take a smaller step-size.
- In the previous cases (and all other cases unless specified otherwise), we take  $ds = 10^{-5}$ .

## Observables

- To emphasize the two major advantages of the Magnus implementation, we now consider evolved observables and operators for the remainder of the section.
- Table I shows the relative error on the deuteron bound state energy and root mean square of all eigenvalues for several evolution cases.
- The Magnus approach preserves energies to several orders of magnitude better than the typical SRG approach.

TABLE I: Relative error on the deuteron bound state energy and the root mean square of eigenvalues where  $\tilde{\epsilon}$  denotes an eigenvalue of an SRG or Magnus evolved Hamiltonian for  $\Lambda = 9 \text{ fm}^{-1}$  and  $\lambda = 1.2 \text{ fm}^{-1}$ .

	$G$	$ \frac{\epsilon_d - \tilde{\epsilon}_d}{\epsilon_d} $	$\sqrt{\frac{1}{N} \sum_i^N (\tilde{\epsilon}_i - \epsilon_i)^2} \text{ [MeV]}$
SRG		$1.165 \times 10^{-5}$	$3.016 \times 10^{-4}$
Magnus, $k_{max} = 2$	$H_D$	$5.010 \times 10^{-10}$	$4.097 \times 10^{-9}$
Magnus, $k_{max} = 14$		$1.206 \times 10^{-11}$	$3.950 \times 10^{-10}$
SRG		$1.003 \times 10^{-4}$	$9.791 \times 10^{-5}$
Magnus, $k_{max} = 2$	$T_{rel}$	$7.775 \times 10^{-8}$	$6.376 \times 10^{-8}$
Magnus, $k_{max} = 14$		$7.607 \times 10^{-8}$	$6.359 \times 10^{-8}$

- Again, despite the inclusion of several more terms in the sum of Eqn. 5, we see consistent errors between  $k_{max} = 2$  and 14 because of the guaranteed unitarity of  $U(s) = e^{\Omega(s)}$
- The errors on the Magnus energies are within the region of floating-point error whereas the SRG compounds error in solving the ODE 2.
- We have also checked the phase shifts from the evolved potentials match the bare potentials in all cases for Magnus and SRG evolution.
- Next we show the evolved deuteron wave function for several cases.
- Figure 5 shows the deuteron momentum probability density,  $|\phi(k)|^2$ , on a semi-log scale as a function of momentum for both band-diagonal generators.
- With  $G = H_D$ , the evolved and un-evolved momentum distributions agree for low-momentum whereas  $G = T_{rel}$  significantly distorts the distribution from the presence of the spurious bound state in the  $\Lambda = 9 \text{ fm}^{-1}$  potential.
- This illustrates the advantage of the Wegner generator: the spurious bound state at high-momentum does not affect the low-momentum physics under the SRG transformation.
- In all cases of Magnus and SRG evolution, we can consistently evolve wave functions and operators to make reliable calculations of observables.
- To demonstrate this, we calculate the deuteron RMS radius and quadrupole moment with the  $\Lambda = 9 \text{ fm}^{-1}$  potential using the Magnus implementation with the Wegner generator.
- The initial values of the chiral potential are  $r_d = 2.022 \text{ fm}$  and  $Q_d = 0.287 \text{ fm}^2$  compared

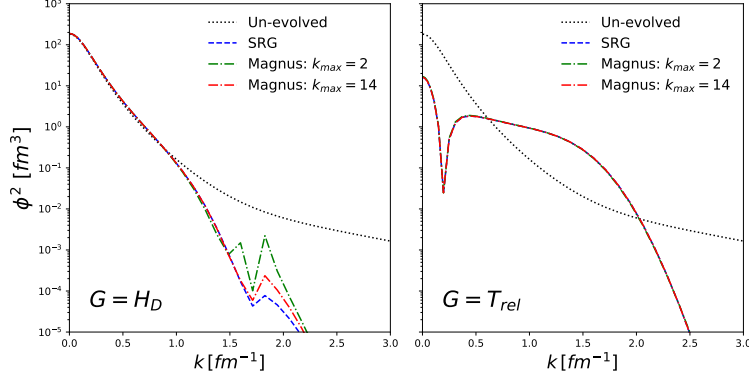


FIG. 5: Momentum probability densities of the deuteron comparing the un-evolved wavefunction (black dotted line), SRG evolved wavefunction (blue dashed line), and two Magnus evolved wavefunctions with truncations 2 and 14 (green and red dash-dotted lines, respectively) where  $\lambda = 1.2 \text{ fm}^{-1}$ . The left panel shows evolution with  $G = H_D$  and the right with  $G = T_{rel}$ . Here  $\Lambda = 9 \text{ fm}^{-1}$ .

to the experimental values  $r_d^{exp} = 2.141 \text{ fm}$  and  $Q_d^{exp} = 0.286 \text{ fm}^2$ .

– We have checked for several cases with the Magnus and found near-perfect agreement to the initial values of both observables.

#### UPDATED UP TO HERE 04/03/19

- RMS radius and quadrupole moment of deuteron.
- Values from initial potential ( $\Lambda = 9 \text{ fm}^{-1}$ ):
  - $r_d = 2.022 \text{ fm}$  (using momentum-space derivatives)
  - $r_d = 2.465 \text{ fm}$  (using Fourier transforms)
  - $Q_d = 0.287 \text{ fm}^2$  (using momentum-space derivatives)
- Values from standard Magnus evolved potential ( $G = H_D$ ,  $\lambda = 1.2 \text{ fm}^{-1}$ , and  $k_{max} = 6$ ):
  - $r_d = 2.022 \text{ fm}$  (using momentum-space derivatives)
  - $Q_d = 0.287 \text{ fm}^2$  (using momentum-space derivatives)s
  - Note: we apply  $U^\dagger(s)U(s)$  to wave function to compute unitarily equivalent observables
- Experimental values:

- $r_d = 2.141 \text{ fm}$

- $Q_d = 0.286 \text{ fm}^2$

## Evolution of operators

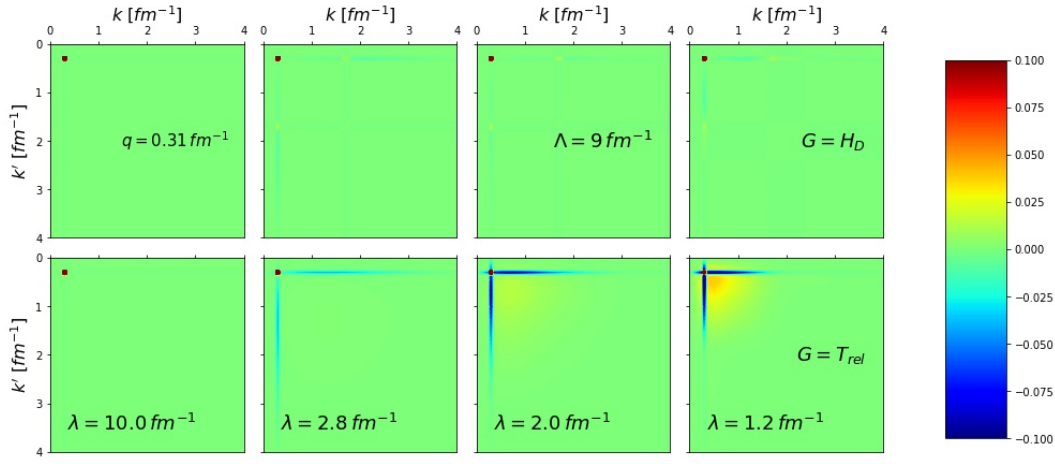


FIG. 6: Matrix elements of  $\langle k | a_q^\dagger a_q | k' \rangle$  Magnus evolving in  $\lambda$  right to left with  $G = H_D$  (top) and  $G = T_{rel}$  (bottom). Here  $q = 0.31 \text{ fm}^{-1}$ ,  $\Lambda = 9 \text{ fm}^{-1}$ , and  $k_{max} = 6$ .

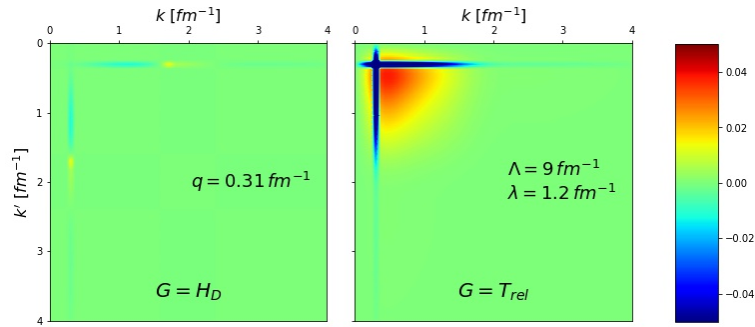


FIG. 7: Difference in evolved and bare matrix elements of  $\langle k | a_q^\dagger a_q | k' \rangle$  Magnus evolving to  $\lambda = 1.2 \text{ fm}^{-1}$  right to with  $G = H_D$  (left) and  $G = T_{rel}$  (right). Here  $q = 0.31 \text{ fm}^{-1}$ ,  $\Lambda = 9 \text{ fm}^{-1}$ , and  $k_{max} = 6$ .

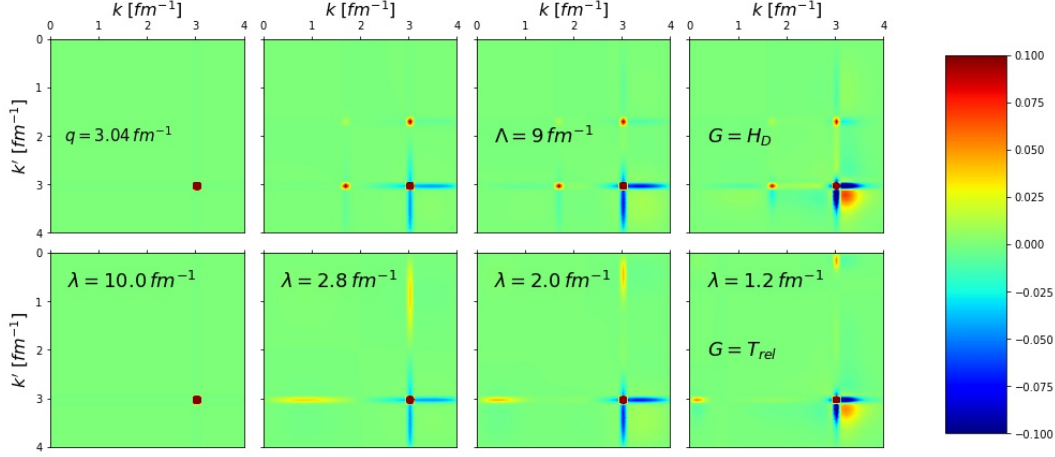


FIG. 8: Matrix elements of  $\langle k|a_q^\dagger a_q|k'\rangle$  Magnus evolving in  $\lambda$  right to left with  $G = H_D$  (top) and  $G = T_{rel}$  (bottom). Here  $q = 3.04 \text{ fm}^{-1}$ ,  $\Lambda = 9 \text{ fm}^{-1}$ , and  $k_{max} = 6$ .

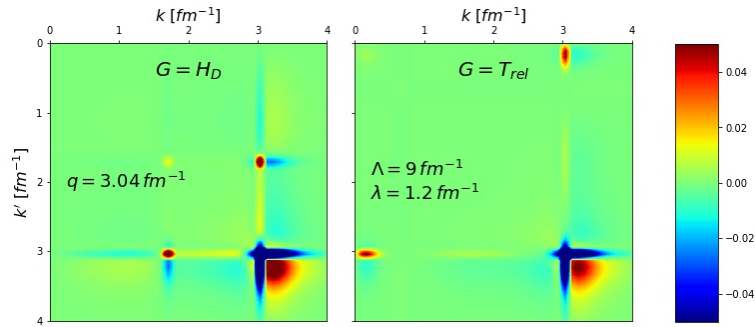


FIG. 9: Difference in evolved and bare matrix elements of  $\langle k|a_q^\dagger a_q|k'\rangle$  Magnus evolving to  $\lambda = 1.2 \text{ fm}^{-1}$  with  $G = H_D$  (left) and  $G = T_{rel}$  (right). Here  $q = 3.04 \text{ fm}^{-1}$ ,  $\Lambda = 9 \text{ fm}^{-1}$ , and  $k_{max} = 6$ .

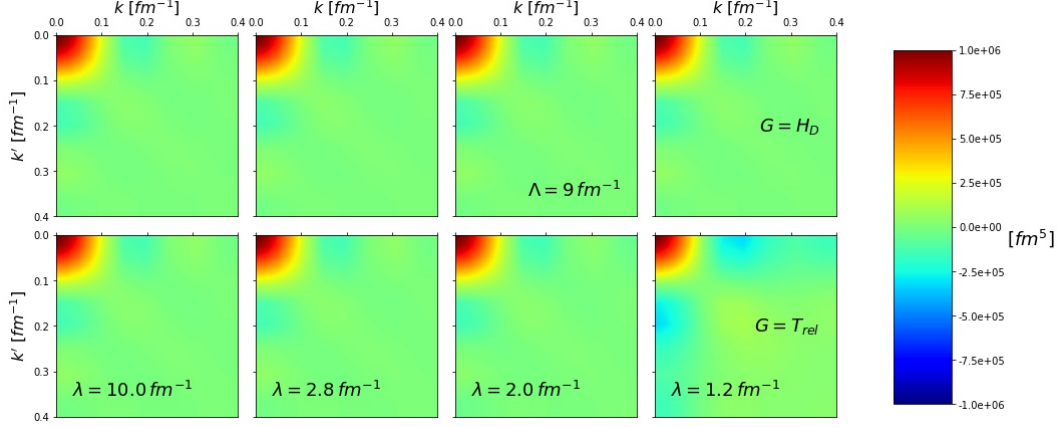


FIG. 10: Matrix elements of  $\langle k|r^2|k' \rangle$  Magnus evolving in  $\lambda$  right to left with  $G = H_D$  (top) and  $G = T_{rel}$  (bottom). Here  $\Lambda = 9 fm^{-1}$  and  $k_{max} = 6$ .

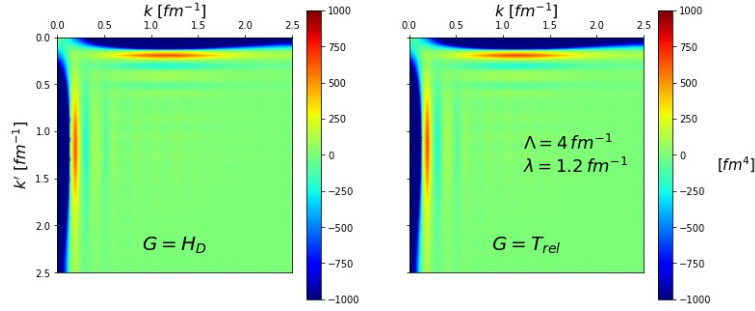


FIG. 11: Difference in evolved and bare matrix elements of  $\langle k|r^2|k' \rangle$  Magnus evolving to  $\lambda = 1.2 fm^{-1}$  with  $G = H_D$  (left) and  $G = T_{rel}$  (right). Here  $\Lambda = 4 fm^{-1}$  and  $k_{max} = 6$ .

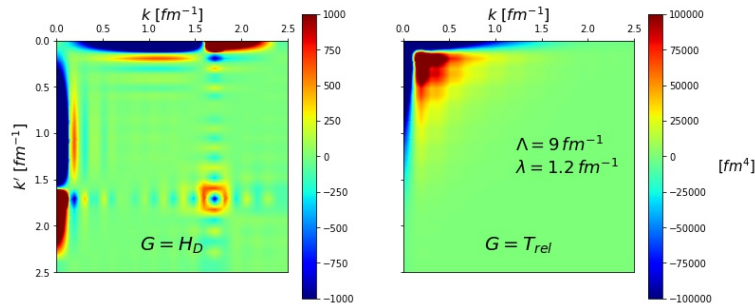


FIG. 12: Difference in evolved and bare matrix elements of  $\langle k|r^2|k' \rangle$  Magnus evolving to  $\lambda = 1.2 fm^{-1}$  with  $G = H_D$  (left) and  $G = T_{rel}$  (right). Here  $\Lambda = 9 fm^{-1}$  and  $k_{max} = 6$ . (Note the difference in color bar scales.)

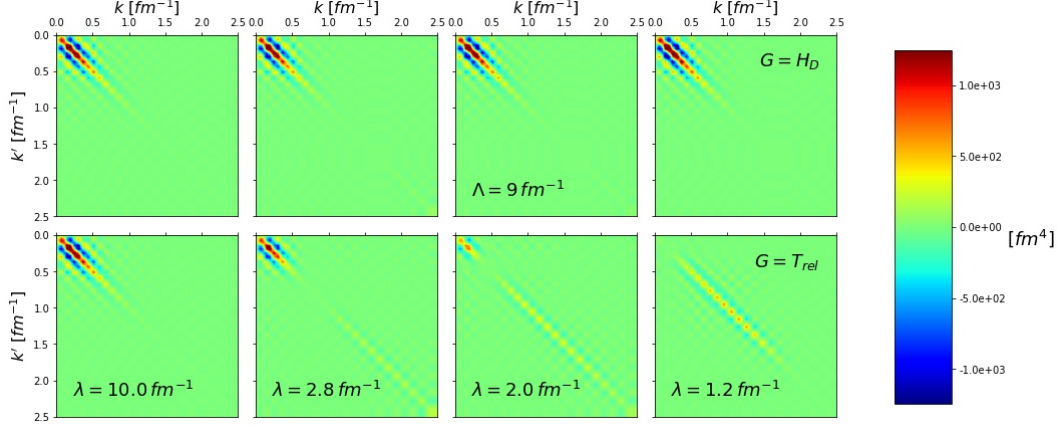


FIG. 13: Integrand of  $\langle \Psi | k \rangle \langle k | r^2 | k' \rangle \langle k' | \Psi \rangle$  Magnus evolving the wave function in  $\lambda$  right to left with  $G = H_D$  (top) and  $G = T_{rel}$  (bottom). Here  $\Lambda = 9 \text{ fm}^{-1}$ ,  $k_{max} = 6$ , and the operator  $r^2$  is un-evolved.

#### IV. CONCLUSION

- Summarize.
- Where does the Magnus implementation differ from the SRG result?
- Connection to the IMSRG intruder state problem.
- Outlook.

- 
- [1] H. Hergert, S. K. Bogner, T. D. Morris, A. Schwenk, and K. Tsukiyama, Phys. Rept. **621**, 165 (2016), arXiv:1512.06956 [nucl-th].
  - [2] H. Hergert, S. K. Bogner, J. G. Lietz, T. D. Morris, S. Novario, N. M. Parzuchowski, and F. Yuan, Lect. Notes Phys. **936**, 477 (2017), arXiv:1612.08315 [nucl-th].
  - [3] T. D. Morris, N. Parzuchowski, and S. K. Bogner, Phys. Rev. C **92**, 034331 (2015), arXiv:1507.06725 [nucl-th].
  - [4] B. Dainton, R. J. Furnstahl, and R. J. Perry, Phys. Rev. C **89**, 014001 (2014), arXiv:1310.6690 [nucl-th].
  - [5] A. Nogga, R. G. E. Timmermans, and U. van Kolck, Phys. Rev. C **72**, 054006 (2005), arXiv:nucl-th/0506005 [nucl-th].
  - [6] S. D. Glazek and R. J. Perry, Phys. Rev. D **78**, 045011 (2008), arXiv:0803.2911 [nucl-th].



- [7] K. A. Wendt, R. J. Furnstahl, and R. J. Perry, Phys. Rev. C **83**, 034005 (2011), arXiv:1101.2690 [nucl-th].
- [8] I. Tews, L. Huth, and A. Schwenk, Phys. Rev. C **98**, 024001 (2018), arXiv:1806.00233 [nucl-th].
- [9] F. Wegner, Annalen der Physik **506**, 77 (1994).
- [10] S. Blanes, F. Casas, J. A. Oteo, and J. Ros, Phys. Rep. **470**, 151 (2009), arXiv:0810.5488 [math-ph].
- [11] W. Magnus, Commun. Pure Appl. Math. **7**, 649 (1954).